




Article

Using Digital Image Analysis to Estimate Corn Ear Traits in Agrotechnical Field Trials: The Case with Harvest Residues and Fertilization Regimes

Dušan Dundžerski ^{1,*} , Goran Jaćimović ² , Jovan Crnobarac ² , Jelena Visković ² and Dragana Latković ^{1,2}

¹ Institute of Field and Vegetable Crops, National Institute of the Republic of Serbia, Maksima Gorkog 30, 21101 Novi Sad, Serbia

² Faculty of Agriculture in Novi Sad, University of Novi Sad, Trg Dositeja Obradovića 8, 21102 Novi Sad, Serbia

* Correspondence: dusan.dundzerski@nsseme.com

Abstract: In this study, we aimed to evaluate the feasibility of digital image analysis (DIA) as a substitute for standard analysis (SA) in assessing corn ear traits in agrotechnical field trials. Accurate and timely prediction of corn yield through corn ear traits can lead to precise agricultural management recommendations for the improvement of production. Four replications with 10 plots each were subjected to different fertilization regimes and analyzed using DIA and SA to determine the kernel number per ear (KN), ear length (EL), and ear diameter (ED). For both methods, the results showed that only nitrogen doses had a significant effect on the examined corn ear traits, and the correlation matrix revealed a strong and significant relationship between yield and corn ear traits. The post-hoc test showed no discrepancy in cases between the two methods for KN and EL, with a 6.7% discrepancy for ED. For both methods, a linear plateau was the best fit for KN and EL with increasing nitrogen doses, whereas a quadratic plateau was the best fit for ED. The regression equations for both methods provided similar recommendations regarding nitrogen requirements. The findings suggest that DIA can be used as a substitute for SA of corn ear traits obtained from different fertilization variants and can provide nitrogen fertilization recommendations for optimal corn yields.



Citation: Dundžerski, D.; Jaćimović, G.; Crnobarac, J.; Visković, J.; Latković, D. Using Digital Image Analysis to Estimate Corn Ear Traits in Agrotechnical Field Trials: The Case with Harvest Residues and Fertilization Regimes. *Agriculture* **2023**, *13*, 732. <https://doi.org/10.3390/agriculture13030732>

Academic Editor: Yanbo Huang

Received: 24 February 2023

Revised: 16 March 2023

Accepted: 19 March 2023

Published: 22 March 2023



Copyright: © 2023 by the authors. Licensee MDPI, Basel, Switzerland. This article is an open access article distributed under the terms and conditions of the Creative Commons Attribution (CC BY) license (<https://creativecommons.org/licenses/by/4.0/>).

Keywords: kernel number; ear length; ear diameter; nitrogen doses; yield; linear plateau; quadratic plateau

1. Introduction

The productivity of a maize genotype, whether it is a hybrid or a variety, depends on both its genetics and the environment in which it grows. Three yield components determine the yield of maize in a specific environment: the number of ears per unit area, the kernel number per ear (KN), and the weight of each kernel. The KN of an ear depends on the number of kernel rows per ear (which is influenced by ear diameter or ED) and the number of kernels per row (which depends on the length of the ear or EL). Changing any of these components while keeping the others constant will result in a corresponding change in grain yield. Therefore, efforts to increase maize yield through agronomic management or breeding strategies should focus on enhancing one or more of these yield components while keeping the others at a constant level [1].

Nitrogen is an essential macronutrient for plants, and it plays a crucial role in maize growth and development. Nitrogen accounts for up to 5% of the total dry matter, and it is a component of various plant substances, such as leaf pigments, amino acids, nucleic acids, proteins, and plant hormones. Nitrogen also plays a vital role in photosynthesis. Reduced nitrogen supply adversely affects various aspects of maize growth and development, including germination, seedling emergence, tillering, flowering, pollination, yield, and grain quality. At the early seedling stage, insufficient nitrogen supply results in poor seedling establishment. In the early vegetative stage, it hampers root and shoot growth, thereby hindering mineral and water uptake and reducing leaf area. Continued nitrogen

deficiency results in decreased photosynthesis, leading to reduced grain yields due to lighter and shorter ears, lighter kernels, and fewer ears produced [2].

The application of less nitrogen reduces grain yield, and KN per ear is a critical indicator of the ear's storage capacity, which is the primary reason for the different grain yields of maize varieties with varying nitrogen efficiency. Low nitrogen stress increases the number of aborted kernels and unpollinated filaments, resulting in a decrease in KN [3]. The authors in [4] found that nitrogen deficiency can reduce KN per ear by up to 41%, whereas sufficient nitrogen supply reduces it by 20%. Different studies have investigated the relationship between nitrogen application levels, grain yield, and nitrogen use efficiency, but results vary considerably due to differences in maize varieties, fertilizer levels, and climatic conditions.

An image is defined as a two-dimensional function, denoted by $f(x, y)$, where x and y represent spatial (plane) coordinates, and the amplitude at any pair of coordinates (x, y) is referred to as the intensity or gray level of the image at that point. When x , y , and the intensity values of f are all finite, discrete quantities, the image is deemed a digital image [5]. The field of digital image analysis (DIA) involves the manipulation of digital images by means of a digital computer, and as such, the historical progression of digital image processing is closely linked to the advancement of the digital computer [5]. Initially, image processing was primarily utilized for enhancing image quality, and one of the first successful applications occurred in 1964 when the Space Detector Ranger 7 captured numerous high-resolution images of the Moon. The Ranger series of spacecraft was specifically designed to capture high-quality images of the Moon and transmit them back to Earth in real time. The images were utilized for scientific analysis, as well as for selecting landing sites for the Apollo Moon missions [6].

In contemporary times, DIA has emerged as a broad and multifaceted field that is applied across a diverse range of domains. The scope of imaging machines spans the electromagnetic spectrum in its entirety, encompassing gamma-ray, X-ray, ultraviolet (UV), visible, infrared (IR), microwave, and radio imaging [7]. The potential applications of digital imaging are numerous and encompass a range of fields, including agriculture [8]. Within the field of agriculture, image processing techniques have been employed in soil [9–11], land [12–14], and crop management [15–18].

According to the Food and Agriculture Organization of the United Nations, the five main grains harvested in 2019 were corn, wheat, rice, soybean, and barley, with a total of over 3.1 billion tons [19]. The utilization of genetic tools and techniques has allowed the development of high-yielding, stress-tolerant plants through genetic selection [20]. However, the increasing demands of the world's growing population require an acceleration of plant breeding programs to achieve higher potential crop yields. The currently utilized phenotyping devices and methods do not offer adequately fast and precise estimations of thousands of recombinant inbred lines; thus, imaging and image processing methods utilizing the visible to the near-infrared range have been developed to provide non-damaging plant phenotype image datasets with increased precision and throughput, as well as high-dimensional phenotype data for the modeling and prediction of plant growth and development [21]. Miller et al. [22] developed and described three custom algorithms designed to automatically measure the sizes, shapes, and numbers of ears and kernels of maize plants from digital images. These algorithms provide an objective and faster alternative to typical manual methods without sacrificing accuracy, as demonstrated by their high correlations with ground truth measurements and simulated data. Khaki et al. [23] proposed a deep learning method called "DeepCorn" for accurately counting ear corn kernels in the field, which can aid in gathering real-time data and improving decision-making to maximize crop yields. They explained that accurately phenotyping crops to record various traits such as color, head count, height, weight, etc., is a bottleneck for commercial organizations that manage large amounts of crops due to limited time and labor. The proposed method uses a truncated VGG-16 as a backbone for feature extraction and merges feature maps from multiple scales of the network to make it robust against image

scale variations. Zhang et al. [24] proposed a method for high-throughput corn ear testing based on capturing image sequences of corn ear samples using a panoramic photography collection system and processing the images to acquire indexes such as lengths, radiuses, rows, and KN per ear. The proposed method showed high accuracy in acquiring these indexes, making it an effective method for corn ear testing in modern corn breeding. Two semi-automatic machine vision methods for counting maize kernels on de-husked ears with varying row morphologies were developed in [25]. The first method mimics a manual field method of estimating total kernel count by counting rows and multiplying by the number of kernels per row. The second method only observes a fixed quasi-cylindrical midsection of the ear, acquiring image frames of individual rows of kernels located in the midsection. The algorithm proposed in [26] comprises five steps and has been tested in field trials using eight maize varieties in China. The results showed good agreement between ground truth (manual counting) values and image-based counting values, making the method applicable and satisfactory for real-world breeding programs.

Alongside breeding, agrotechnical operations to support high-yielding plants must also be studied. Agrotechnical field trials with independent factors, such as crop rotations, fertilizer rates and tillage systems, seeding times and rates, and plant densities, provide valuable information on fully expressing the genetic potential of the created genotypes. However, the complexity of trials, the number of independent factors and variants, the number of genotypes being examined, and the number of examined traits indicate the need for the faster determination of traits in comparison to standard methods. The determination of plant yield components across and between independent factors and variants is particularly time-consuming and subjective, with the current methods relying on hiring a large number of workers for measurements [27].

To address this issue, the standard practice in corn research has been to take a small subsample of plants, usually ten plants [28–32], or from a specific area in the plot [30,33], which may potentially increase random error. Random error can be reduced by increasing sampling variability and sample size [34]. In research, bias occurs when “systematic error is introduced into sampling or testing by selecting or encouraging one outcome or answer over others” [34]. Digital image analysis can greatly reduce the time required for analysis and enable the analysis of more samples per plot while keeping the analysis consistent and uniform throughout the entire process. We can also save samples in a digital format for an unlimited time, and new algorithms can be developed for future image analysis.

The devices currently available for KN estimation, such as corn shellers and electromagnetic vibration boxes, are expensive, single-function devices, and are thus relatively impractical. The measurement of corn ear dimensions using a ruler or calipers is a slow process. Proposals for the DIA of corn ear traits in plant breeding field trials have mostly been based on correlation and regression models between image-based and manually determined corn ear traits. However, to our knowledge, no studies have been conducted to examine whether image-based corn ear traits provide similar results to those of manually determined corn ear traits in agrotechnical field trials using methods that describe the relationship between crop traits and agricultural variants. There are several of these methods. The most common are regression and correlation analysis, analysis of variance (ANOVA), and the analysis of statistical differences between group means (post-hoc tests).

Regression analysis describes the effect of one or more variables (designated as independent variables) on a single variable (designated as the dependent variable) by expressing the latter as a function of the former. Correlation analysis, on the other hand, provides a measure of the degree of association between the variables or the goodness of fit of a prescribed relationship to the data at hand. Regression and correlation procedures can be classified according to the number of variables involved and the form of the functional relationship between the dependent variable and the independent variables. The procedure is referred to as simple if only two variables (one dependent and one independent variable) are involved; otherwise, it is referred to as multiple. The procedure is termed linear if the form of the underlying relationship is linear; otherwise, it is referred to as nonlinear [35]. In

certain situations in agricultural research, especially those of soil fertility and soil chemistry, the response function exhibits a plateau effect. In such situations, it is often appropriate to approximate the underlying function with two intersecting linear lines accounting for the sloping as well as the plateau segments of the response [36]. This is known as linear-plateau regression and its use in evaluating responses to fertilizer nutrients was first introduced in [37]. A quadratic plateau model is similar to a linear plateau model, except that the linear segment is replaced with a quadratic function. The quadratic-plateau model best described the observed yield response in the study presented in [38]. Analysis of variance (ANOVA) is a statistical technique used to analyze variations in a response variable (continuous random variable) measured under conditions defined by discrete factors (classification variables, often with nominal levels) [39]. The main issue related to applying ANOVA tests is that the method does not tell the experimenter which pair in the population has a different mean when the null hypothesis is rejected. To overcome this issue, post-hoc multiple comparison tests can be applied to determine which pair of the population has a different population mean [40].

In this study, we aimed to examine whether image-based corn ear traits provide similar and faster results than manually determined corn ear traits using the most common and essential statistical analyses used in agrotechnical field trials. The future implications of this study concern the accurate and timely prediction of corn yields on the basis of corn ear traits before mechanical harvesting and precise agricultural management recommendations for the improvement of production. Estimating corn yields in agrotechnical field trials before a mechanical harvest is important from a scientific and practical standpoint. It helps researchers evaluate the effectiveness of different treatments and interventions and helps farmers identify the most effective inputs and management practices for their particular growing conditions. Furthermore, there is a possibility that a hailstorm or strong wind could destroy the agrotechnical field trial before it is mechanically harvested. By determining corn ear traits using image analysis before harvesting, we can estimate corn yields and obtain precious information that would be lost otherwise.

2. Materials and Methods

2.1. Site and Experimental Design

The trial was conducted at the Institute of Field and Vegetable Crops in Novi Sad (Vojvodina Province, Serbia) in a long-term stationary field trial on chernozem soil, classified as A–C class (humus accumulative soils). The rotation of soybean, wheat, and corn was used in this trial, with corn following wheat. Each crop occupied an area of 0.24 ha (68 m by 34 m), with four replications in each area, consisting of 10 plots and different fertilization treatments in one replication. The fertilization treatments included:

1. Harvest residue (HR) ploughing with \emptyset (control), 50, 100, 150, 200, and 250 kg nitrogen (N) ha^{-1} ; and
2. Without HR ploughing with \emptyset (control), 100, and 200 kg N ha^{-1} .

The design of the experiment was an unbalanced split-plot design, in which whole plots were harvest residues, and subplots were nitrogen doses. Before winter plowing, the entire amount of phosphorus (as monoammonium phosphate, 80 kg ha^{-1}) and potassium (as potassium chloride, 80 kg ha^{-1}) was added manually, along with 50% of the nitrogen (as ammonium nitrate). The remaining nitrogen (as ammonium nitrate) was added manually in the spring before cultivation and sowing. Three maize hybrids, NS 770, NS 640, and NS 4024, were sown on each plot with four rows, spaced 0.75 m apart using a Nodet Pneumassem planter. Sowing was carried out on 29 April at an optimal time according to the conditions of Vojvodina. All common agricultural practices for the growing of corn were applied during vegetation. For further ear trait analysis, NS 4024 was chosen. It was hand-harvested at physiological maturity by picking up ears from two middle rows (5 m in length). The harvesting of the other hybrids was carried out using a Wintersteiger harvester. The ears of NS 4024 were put in bags and measured to determine their weight. After that,

5 representative normal ears from each bag were chosen for DIA to determine KN, EL, and ED, and to compare the results with those of SA for these corn ear traits.

2.2. Image Acquisition

In this study, a total of 200 ears were subjected to photographic analysis. This was achieved by utilizing 5-step house ladders as a platform for the camera, with the legs of the ladder maximally spread. A piece of styrofoam was prepared by trimming the edges on the longer side to fit through the ladder, and the center was measured and drilled to match the diameter of the camera objective. The styrofoam was then pulled through the ladder to the third step and the camera was placed in a previously made center hole, maintaining a distance of 62 cm between the objective and the ground.

In diffuse light conditions, we conducted external ear imaging. Nadir images were captured using a Canon EOS 2000D camera with a resolution of approximately 24.7 megapixels. The camera was set to automatic mode with automatic focus and the image quality was set to S2 (1980 × 1280 pixels), resulting in a range of 1 to 1.74 megabytes per picture. A black shirt was utilized as the background, on which all five ears from a single bag were placed and photographed. Prior to image acquisition, the shirt was tightly secured to prevent any color discrepancies in the background. The ears were carefully positioned to avoid contact with one another, together with a card containing the fertilizer variant and repetition number. A 30 cm ruler was inserted before photographing the corn to enable the conversion of pixel measurements to centimeters (Figure 1). The Canon Connect application facilitated indirect image capture from a smartphone. Following each image capture, the ears were stored in plastic bags with the corresponding card and numbered 1 to 5 based on their location in the image. The original images are available for download upon request.



Figure 1. Example image of five ears of corn taken from one fertilizer variant.

Upon completion of the image capture process, EL and ED were measured, utilizing a digital caliper, with a precision of two decimal places, in accordance with the guidelines outlined in [41]. Subsequently, ears were shelled using an electric sheller that ensured the preservation of every kernel and cob. To facilitate subsequent analyses, kernels from a given ear were consolidated within the corresponding plastic bag. This enabled the comparison

of kernel counts derived from the captured images and a kernel counter (Contador, Pfeuffer GmbH, Kitzingen, Germany). The duration of each step is reported in Table 1.

Table 1. Total times needed for each step in the process.

Method	Process	Time for 200 Ears *
SA ¹	To manually determine and write down EL and ED, and count ear rows	4 h and 30 min
	To shell ears, collect their kernels, and put them in the correct plastic bag	3 h and 20 min
	To count 1000 kernels on a kernel counter	5–6 min
	To count the total number of kernels (75,806 kernels)	7 h and 30 min
	Total	15 h and 20 min
DIA ²	To take ear images (+bring bags with ears, choose ears for photograph, clear silk from ears)	2 h and 30 min
	To determine KN from images	30 min
	To determine EL and ED from images	16 min
	Total	3 h and 16 min

* One person performed DIA and measured ear length (EL) and ear diameter (ED); more people helped with kernel counting using Contador; the time needed to obtain ear images could be improved by placing more ears in the background and increasing the field of view; we used a smaller number of ears and a decreased field of view simply because we did not have large enough black background. ¹ Standard analysis (SA); ² digital image analysis (DIA).

The kernel and cob weight of each ear were measured with a digital scale that provided a precision of two decimal points. Subsequently, the kernels were combined, and a 100 g portion of the composite was utilized for the determination of moisture content. The measurement of moisture content was conducted by subjecting the samples to constant heat in an oven and measuring the weight loss. Kernel weight and yield were standardized to a moisture content of 14%. We calculated yield ($t\ ha^{-1}$) using Equation (1):

$$\text{Yield} = \frac{a * b}{0.86} * \frac{1333.33}{1000} \quad (1)$$

where a = kernel yield per plot in kg, b = % dry matter, 1333.33 is the correction factor to estimate yield per ha from yield per plot ($10.000\ m^2/\text{plot length} \times \text{row width} \times 2$), and 1000 is the number needed to convert kg to t.

2.3. Image Analysis

The images in the Joint Photographic Experts Group (JPEG) format were transferred to a computer and analyzed with a program named Fiji/ImageJ version 1.53c, an image processing package that contains many plugins to facilitate scientific image analysis. Makanza et al. [42] presented a simple and understandable description of the process to prepare images for the determination of KN, EL, and ED; therefore, we followed their algorithm. For KN, to ensure accurate segmentation, a threshold of 100 was chosen for pixel subtraction. This helped to eliminate background pixels with similar color intensities as kernels, reducing the likelihood of significant noise during the process. We employed the contrast-limited adaptive histogram equalization (CLAHE) technique to improve kernel edge visibility while suppressing surface noise. Further enhancement of the edges was achieved by applying the unsharp mask method with a radius of 5 and a mask value of 0.70. We then converted the image to an 8-bit format for ease of processing. Although some low-contrast artifacts were still present after edge detection, we utilized the Phansalskar local threshold method, which is a modification of Sauvola's method, to overcome this issue. This method has proven to be highly effective in cytological images with low contrast. Following binarization, we filled any holes in the image to ensure solid kernel shapes, preventing any splitting during the adjustable watershed step. The adjustable watershed is a plugin that provides the flexibility to adjust the tolerance level to suit the smoothness and shape of the kernel edges, allowing for more accurate segmentation [42]. The parameter values of each step are given in the S1 File, in the Supplementary Materials.

We made small changes to the process described in [42] to determine KN—we removed outliers in the image during the binarization process (Process > Noise > Remove Outliers, with the radius set to 3, the threshold to 50, and bright particles removed). Outliers were mainly small particles such as dust and chaff that were left on the black background after switching ears.

For EL and ED, kernels were filtered out via a Gaussian blur method. This filter uses convolution with a Gaussian function for smoothing. This was followed by a binarization step with the filling up of holes [42]. Instead of the minimum bounding box of a region of interest, which was the method used by [42], we used MinFeret to obtain ED, since the first method did not provide good results. The reason for this was that some ears were not placed in exact alignment with the Y-axis of the image; therefore, the ED was oversized. MinFeret is a measure of the particle's width that is not dependent on ear position. It is called the minimum caliper diameter, defined as the shortest distance between two parallel planes touching the particles on opposite sites for any orientation of the particle. The Feret diameter, also known as a maximum caliper diameter, which is the longest distance between two points on the boundary of the region of interest, was used for EL measurements. As shown in Figure 2, which depicts the results tab, the starting coordinates of the Feret diameter (FeretX and FeretY) are displayed. In addition to this, the FeretAngle (0–180 degrees, the angle between the Feret diameter and a line parallel to the x-axis of the image) is shown, which, together with the FeretX, FeretY, and the length of the Feret diameter, can be used to draw the Feret diameter of the region of interest, following the macro on Figure 2. Goriewa-Duba et al. [43] recently used Feret and MinFeret, along with other shape descriptors, in order to determine wheat grain length and diameter. The macro used for image analysis is given in the S1 File, in the Supplementary Materials.

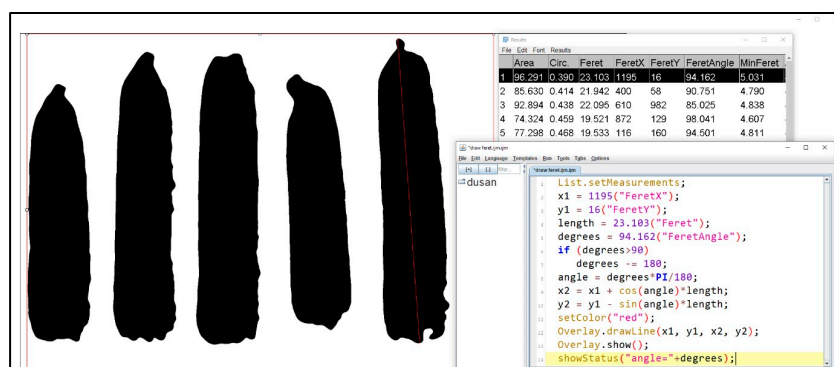


Figure 2. The same ears as those shown in Figure 1, after Gaussian blur filter and binarization were implemented; Feret = ear length, FeretX and FeretY = starting coordinates, FeretAngle = angle between the Feret diameter and a line parallel to the x-axis of the image, MinFeret = ear diameter. The red line on the last ear represents the Feret diameter, and the macro used to draw the Feret diameter is displayed at the bottom right.

2.4. Statistical Analysis

In this study, we conducted linear regression analysis to compare the results obtained through SA and DIA for KN, EL, and ED. The linear equations were then used to estimate these corn ear traits. Linear regression analysis assumes that there is a linear relationship between the predictor variable(s) and the outcome variable. We used residual plots to check for deviations from linearity. The residuals were evenly distributed around zero and did not form any distinct patterns. Linear regression analysis can be sensitive to outliers, which can have a disproportionate impact on the results. We used the box-plot method to check for outliers (they were defined as observations that were more than 1.5 times the interquartile range (IQR) above the upper quartile or below the lower quartile). The variance of the outcome variable must be constant across all levels of the predictor variable(s) in linear regression analysis. We used residual plots to check for deviations

from homoscedasticity. The residuals did not show a pattern of increasing or decreasing variance as the predictor variable(s) increased. The assumption of normality refers to the assumption that the residuals are normally distributed. The normality of residuals was validated via the Shapiro–Wilk test.

Additionally, Lin's concordance correlation coefficient (r_c) was used to compare the two methods [44], which was interpreted in conjunction with the simple correlation coefficient. Lin's concordance correlation coefficient (r_c) is especially important when introducing a new measurement capability that has some advantages (e.g., less expensive, less time-consuming, safer to use) over an existing measurement technique. The Pearson correlation coefficient measures a linear relationship but fails to detect any departure from the 45° line. Lin's concordance correlation coefficient evaluates the agreement between two readings from the same sample by measuring the variation from the 45° line through the origin (the concordance line). We calculated r_c between two random variables x and y using Equation (2) [42]:

$$r_c = \frac{2rS_xS_y}{\left(\bar{X} - \bar{Y}\right)^2 + s_x^2 + s_y^2} \quad (2)$$

where r is Pearson's correlation coefficient; s_x and s_y are the variances of population X and Y , respectively; and \bar{X} and \bar{Y} are the means of population X and Y . To calculate the confidence interval (CI) for r_c , we applied the Fisher transformation to r_c to get r'_c (Equation (3)):

$$r'_c = \frac{1}{2} \ln \frac{1+r}{1-r} = \frac{\ln(1+r) - \ln(1-r)}{2} \quad (3)$$

Then we used the following standard error (se) for the transformed value (Equation (4)):

$$se(r'_c) = \sqrt{\frac{1}{n-2} \left[\frac{(1-r^2)r_c^2}{(1-r_c^2)r^2} + \frac{2(1-r_c)r_c^3u^2}{(1-r_c^2)^2r} - \frac{r_c^4u^4}{2(1-r_c^2)^2r^2} \right]} \quad (4)$$

where $u = \frac{\bar{X} - \bar{Y}}{\sqrt{s_x s_y}}$

The CI for the transformed value of r_c is then:

$$r'_c \pm z_{crit} se(r'_c)$$

Taking the inverse Fisher transformation produces the desired CI for r_c (Figure 3, first row). The data and formulas used for the calculation of r_c are given in the S2 File, in the Supplementary Materials.

The strength of the relationship between the two methods was further evaluated through the F-test, RMSE (root mean square error) as defined in Equation (5) [45], R^2 (coefficient of determination), and MAPE (mean actual percentage error) as defined in Equation (6) [45].

$$RMSE = \sqrt{\frac{1}{n} \sum_{i=1}^n (X_{ai} - X_{mi})^2} \quad (5)$$

$$MAPE = \frac{1}{n} \sum_{i=1}^n \frac{|X_{ai} - X_{mi}|}{X_{mi}} * 100\% \quad (6)$$

where x_{mi} is the manually measured value, x_{ai} is the automatically measured value, and n is the number of maize samples.

Where possible (when data were given in the form of numbers), then RMSE and MAPE were also calculated for other research papers where DIA was used for the corn ear traits measured here, for comparison purposes. To compare the influence of independent factors on corn ear traits obtained through the two methods, we performed an unbalanced ANOVA and the Fisher least significant difference (LSD) test with a 95% confidence interval

to identify statistical differences between group means. The data analysis and graphical representations were carried out using XLSTAT, a statistical add-in for Microsoft Excel, and OriginPro v. 9.0. The Nutritional Response Model (NRM), version 1.0, an alternative tool for fitting nutritional response models, was used to obtain the best-fitted models for KN, EL, and ED. The NRM tool, developed using the widely available Microsoft Excel software, allows for simultaneous fitting and side-by-side comparisons of several popular models. In comparison to PROC NLIN of SAS, the NRM.xls workbook provided similar results, as demonstrated in the study presented in [46] that compared the broken line, saturation kinetics, 4-parameter logistics, sigmoidal, and exponential models.

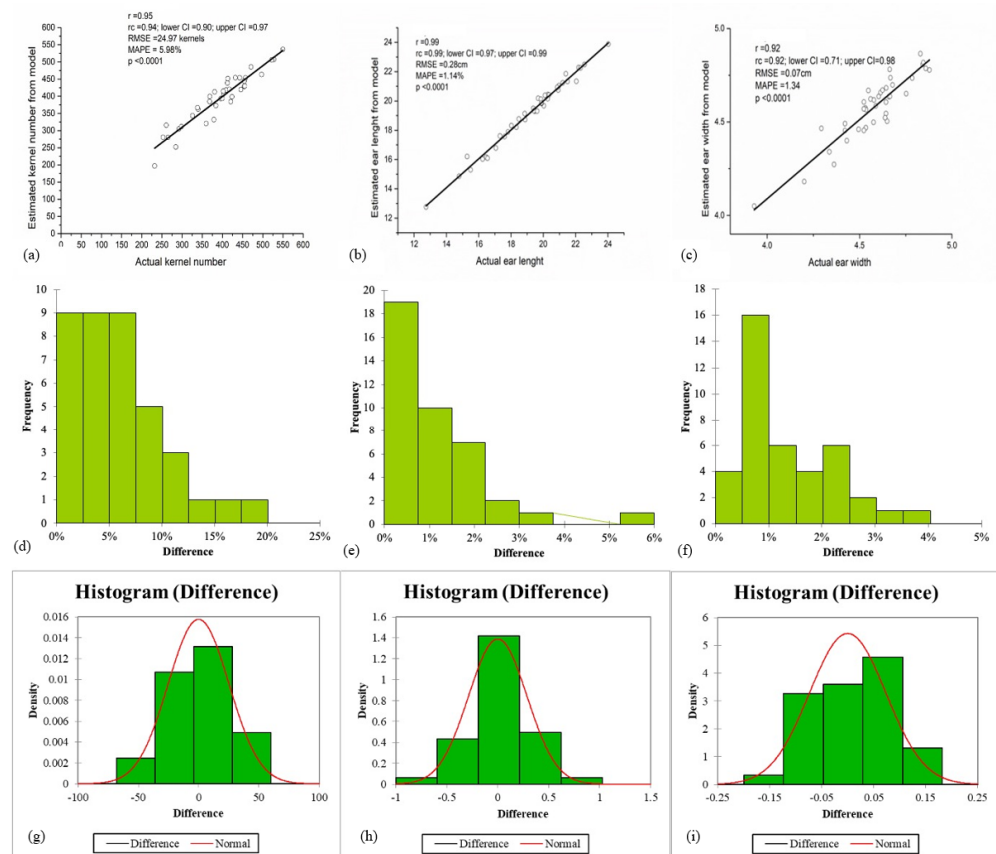


Figure 3. Plots of the relationship, frequency of differences, and normality of differences between the two methods. First row—(a) the relationship between actual KN and estimated KN; (b) actual EL (cm) and estimated EL (cm); (c) and actual (cm) and estimated ED (cm); r = Pearson’s correlation coefficient; r_c = Lin’s concordance correlation coefficient with lower and upper confidence intervals (CI); RMSE = root-mean-square error; MAPE = mean actual percentage error; statistically significant at $p < 0.0001$. Second row—(d) frequency number plots of the differences between estimated and the actual KN; (e) frequency number plots of the differences between estimated and the actual EL; (f) frequency number plots of the differences between estimated and the actual ED. Third row—distribution plot of differences between measurements of two methods for: (g) KN, (h) EL, (i) ED; The red line represents a normal distribution; the Shapiro-Wilk test was used to validate normality for all differences (p -value for KN differences $p = 0.34$, for EL $p = 0.18$, for ED $p = 0.68$).

3. Results and Discussion

3.1. Kernel Number, Ear Length, and Ear Diameter Models

The KN model was estimated based on the relationship between actual KN, obtained with the kernel counter, and KN from the visible part of the ear on the image. The total number of kernels from the image was estimated with a linear equation between the average values of five ears per repetition per variant (total 40 points) on the X and Y axis (read additional comments in the S2 File in the KN spreadsheet, in the Supplementary Materials).

The data showed a linear correlation ($r = 0.95$, $p < 0.0001$) between the KN values estimated using the model (Equation (7)) and the actual counts of detached kernels determined using the kernel counter (Figure 3a, first row).

$$y = 2.1522x - 75.739 \quad (7)$$

We used the same ears for KN validation to compare manual measurements of EL and ED with those generated through the image processing method. The model for the calculation of EL (Equation (8)) and ED (Equation (9)) was obtained in the same way as the KN model.

$$y = 1.0055x - 0.846 \quad (8)$$

$$y = 0.7355x + 1.0967 \quad (9)$$

The data presented a correlation between the two methods for both EL ($r = 0.99$, $p < 0.0001$) and ED ($r = 0.92$, $p < 0.0001$) (Figure 3b,c, first row).

The MAPE values for KN, EL, and ED were 5.98%, 1.14%, and 1.34%, respectively. The RMSE values for KN, EL, and ED were 24.97 kernels and 0.28 and 0.07 cm, respectively. The R^2 values for KN, EL, and ED were 0.90, 0.99, and 0.84, respectively. In Figure 3, in the first row, we can see that the r_c values for KN, EL, and ED were 0.94, 0.99, and 0.92, respectively. Similar results for r_c were obtained in [42], where $r_c = 0.97$, $r_c = 0.97$, and $r_c = 0.95$, for KN, EL, and ED, respectively. Even though they used a much higher camera resolution of 16.2 megapixels for image acquisition, only a slightly higher r_c was obtained in their work.

According to the frequency plots (Figure 3, second row), all absolute percentage errors for KN, EL, and ED were less than 20%, 6%, and 4%, respectively. At the first sight, it is obvious that there was an outlier (5.88% or 0.93 cm) in the frequency plot for EL. In addition, that image was checked. The outlier appeared because the last ear touched the card with the fertilizer variant during the shooting; thus, they were merged after binarization, which caused a surplus in the EL. To consider the use of DIA as a substitute for SA of corn ear traits, the distribution of the differences between the two methods was plotted and the results showed that the differences were normally distributed [47] (Figure 3, third row). We performed a linear regression, with the differences in the measurements as the dependent variable and the average of the measurements as the independent variable, which showed that the bias of differences between methods was not significant, which means that it did not follow any specific trend [47] (S3 File, Supplementary Material).

Miller et al. [22] measured EL and maximum ED using the smallest bounding box method and obtained R^2 values of 0.99 for both measured parameters using a flatbed document scanner. The advantage of this approach is controlled lighting conditions and a fixed background, which enables good quality images. However, a flatbed document scanner requires a computer and power for operation, and may not be appropriate for a large number of corn ear samples, as ears should be brought to the laboratory from outside, which increases the workload. Likewise, a lower number of ears fits in the imaging deck of a flatbed document scanner than in the field of view of a digital camera, and the scanning process is slower than that of image capture. Khaki et al. [23] used a digital camera to obtain corn ear images and determined KN with the use of the deep crowd algorithm [48] and the new algorithm they proposed. The correlation and RMSE values were 0.93 and 45.29, respectively, between the deep crowd algorithm and the ground-truth KN, and 0.96 and 33.11, respectively, between their new algorithm and the ground-truth KN. The importance of their work lies in the use of in situ images, with uncontrolled lighting conditions and a natural background. However, they used the detection-based approach, using a convolutional neural network for kernel detection. As a type of deep learning method, it needs a large amount of training data for successful application [49], requires a fixed distance between ears and the camera, and is not invariant to the ear orientation and the kernel color. Their sliding window approach also increased the inference time and involves a complex and expensive algorithm for the average user, since it requires

strong computational power for training [50]. Zhang et al. [24] proposed a new algorithm using a rotating device for ear and kernel attributes based on panoramic images, called the scale-invariant feature transform algorithm. They obtained good accuracy for KN (RMSE = 16.38 kernels, MAPE = 2.11%) and EL (RMSE = 1.27 cm, MAPE = 5.48%). They used a small sample ($n < 30$) and specified that more data should be used for validating the proposed algorithm. Grift et al. [25] used a rotating device to capture full-length, and quasi-cylindrical mid-section images of ears of corn. For the full-length ears, the correlation between the manually counted versus the machine-vision-estimated numbers of kernels was 0.83, with RMSE = 24.12 kernels and MAPE = 3.45%. The quasi-cylindrical mid-section counting method correlation was 0.98 (no data were given, so RMSE and MAPE could not be calculated). The authors stated that since these methods were used to estimate different measures, no comparison between them was valid. Wu et al. [26] worked on an algorithm that showed good precision under natural and artificial lighting and can be used for different maize varieties. The results showed good agreement (>93%) in terms of accuracy between the ground truth (manual counting) and the image-based counts; nonetheless, it should be mentioned that the KN was counted on only one side of the ear, without the use of a model that estimated the total number of kernels per ear. These and other authors compared their methods with SA of corn ear traits and suggested their use for breeding purposes. However, to our knowledge, no investigations have been performed on the use of DIA of corn ear traits in agrotechnical field trials, where production recommendations based on results need to be given, and in which many other independent factors in addition to corn varieties can be included. This is why we aimed to deepen this field of research and used DIA to examine the behavior of some corn ear traits in response to nitrogen doses (N) and harvest residues (HR).

3.2. Comparison of ANOVA, Post-Hoc Test, Regression Analysis, and Correlation Matrix Results between Methods

After performing unbalanced ANOVA on the data, both methods showed that only nitrogen doses had a statistically significant effect on KN, EL, and ED, with a 95% confidence level (Table 2).

Based on the post-hoc tests of HR results obtained using the two methods, all of the cases showed the same statistical differences for KN, EL, and ED. The least significant difference (LSD) was 32.3 for the actual KN and 31.72 for the estimated KN; the LSD for the actual EL was 1.06, whereas for the estimated EL it was 1.04; and the LSD was 0.11 for the actual and estimated ED. Based on the post-hoc test results of nitrogen doses from two methods used for KN comparisons, all of the cases showed the same statistical differences (Figure 4a), with an LSD of 55.94 for actual KN and an LSD of 54.95 for estimated KN. Post-hoc test results of nitrogen doses on EL matched perfectly for both methods (Figure 4b), with an LSD of 1.83 for actual EL and an LSD of 1.79 for estimated EL. For the ED (Figure 4c), the discrepancy was observed in 6.7% of the cases, between 0 kg N ha⁻¹ and 50 kg N ha⁻¹—with a difference of 0.10 cm between methods (Table 3). The LSD was 0.19 for the actual ED and 0.18 for the estimated ED. The post-hoc test of the interaction of HR × N doses showed small differences between the two methods, 5.5% of cases for the KN, with an LSD of 68.51 for the actual KN, and an LSD of 67.30 for the estimated KN. For the ED, the differences between the two methods were in 8.3% of the cases, with an LSD of 0.23 for the actual ED, and an LSD of 0.22 for the estimated ED. Post-hoc test differences did not occur between methods for the EL within the interaction of HR × N doses (all statistical differences are in S4 File, Supplementary Material). We speculate that these results could be improved using a higher resolution in image acquisition, and by processing image formats that contain minimally processed data from the image sensor (such as the RAW format). It should be noted that the processing time would certainly increase with these changes, depending on the computational power. In this case, we used an AMD Ryzen 5 2600 processor, an RX VEGA 56 8 GB graphics card, and 16 GB RAM on 3200 MHz.

Table 2. Comparison of ANOVA results for KN, EL, and ED between methods.

(1a)					
Source	DF	Sum of squares	Mean squares	F	Pr > F
HR	1	3612.73	3612.73	1.64	0.21 ^{ns}
N doses	5	100,354.43	20,070.89	9.11	<0.01 ^{**}
Repetition	3	23,127.45	7709.15	3.5	0.03 [*]
HR × N doses	2	170.35	85.17	0.04	0.96 ^{ns}
Residual	24	52,896.96	2204.04		
Total	35	180,161.93			
(1b)					
Source	DF	Sum of squares	Mean squares	F	Pr > F
HR	1	1047.45	1047.45	0.49	0.49 ^{ns}
N doses	5	97,966.91	19,593.38	9.21	<0.01 ^{**}
Repetition	3	17,923.7	5974.57	2.81	0.06
HR × N doses	2	1121.54	560.77	0.26	0.77 ^{ns}
Residual	24	51,031.02	2126.29		
Total	35	169,090.61			
(2a)					
Source	DF	Sum of squares	Mean squares	F	Pr > F
HR	1	5.22	5.22	2.22	0.15 ^{ns}
N doses	5	83.81	16.76	7.11	<0.01 ^{**}
Repetition	3	19.7	6.57	2.79	0.06 ^{ns}
HR × N doses	2	0.95	0.48	0.2	0.82 ^{ns}
Residual	24	56.55	2.36		
Total	35	166.23			
(2b)					
Source	DF	Sum of squares	Mean squares	F	Pr > F
HR	1	6.11	6.11	2.7	0.11 ^{ns}
N doses	5	84.26	16.85	7.43	<0.01 ^{**}
Repetition	3	21.56	7.19	3.17	0.04 [*]
HR × N doses	2	0.89	0.44	0.2	0.82 ^{ns}
Residual	24	54.41	2.27		
Total	35	167.23			
(3a)					
Source	DF	Sum of squares	Mean squares	F	Pr > F
HR	1	0.03	0.03	1.25	0.27 ^{ns}
N doses	5	0.5	0.1	4.06	<0.01 ^{**}
Repetition	3	0.05	0.02	0.65	0.59 ^{ns}
HR × N doses	2	0.04	0.02	0.72	0.49 ^{ns}
Residual	24	0.59	0.02		
Total	35	1.21			
(3b)					
Source	DF	Sum of squares	Mean squares	F	Pr > F
HR	1	0.02	0.02	0.89	0.36 ^{ns}
N doses	5	0.37	0.07	3.14	0.03 [*]
Repetition	3	0.08	0.03	1.14	0.35 ^{ns}
HR × N doses	2	0.02	0.01	0.37	0.69 ^{ns}
Residual	24	0.56	0.02		
Total	35	1.05			

(1a)—actual KN; (1b)—estimated KN from model; (2a)—actual EL; (2b)—estimated EL from model; (3a)—actual ED; (3b)—estimated ED from model; HR—harvest residues; N—nitrogen; ** statistically significant at $p < 0.01$; * statistically significant at $0.05 < p < 0.01$; ns not significant.

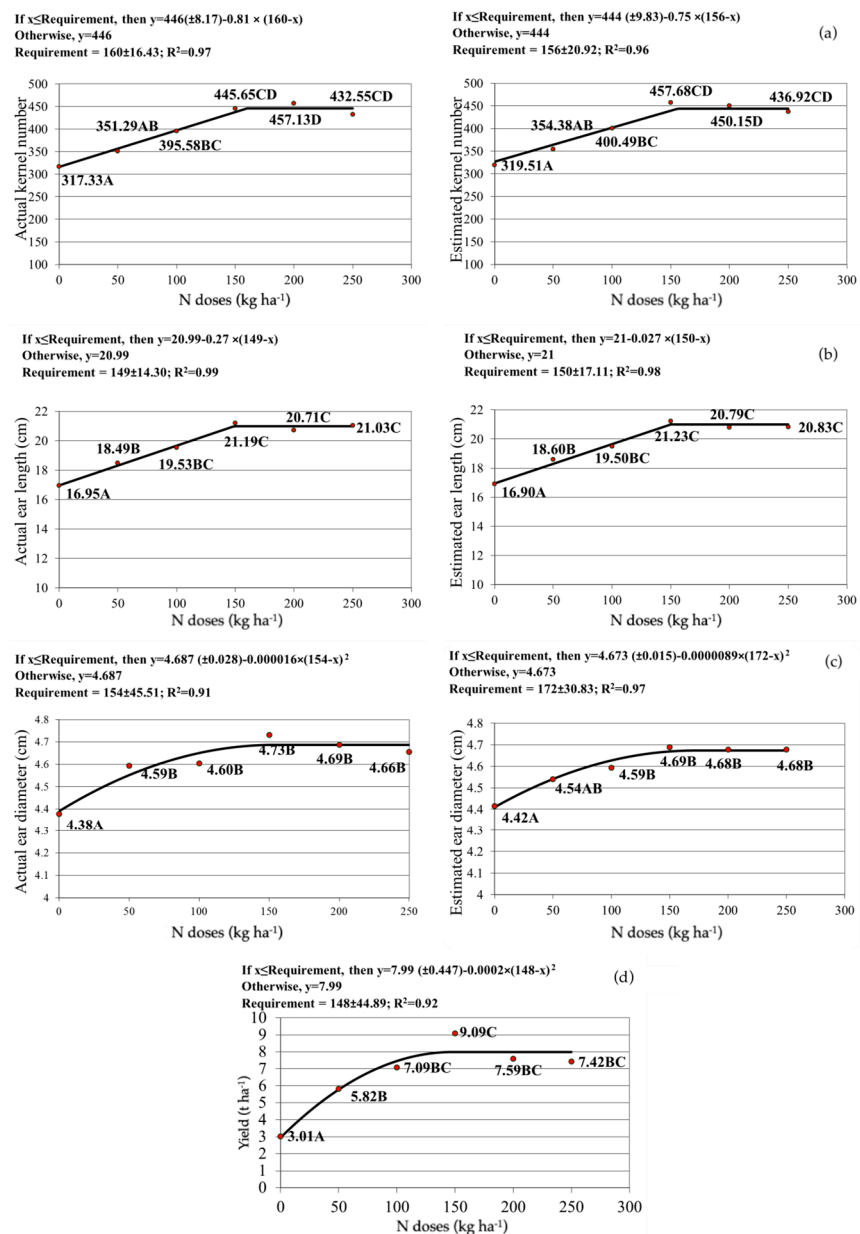


Figure 4. Comparison of the fitted models with increasing nitrogen doses for (a) actual KN and KN estimated using the model; (b) actual EL and EL estimated using the model; (c) actual ED and ED estimated using the model; (d) fitted model for yield with increasing nitrogen doses.

Table 3. Fisher LSD test of nitrogen doses of the differences between group means that showed statistical difference.

Contrast	Difference (Actual)	$p > \text{Diff}$	Difference (Estimated)	$p > \text{Diff}$
0 kg N ha ⁻¹ vs. 50 kg N ha ⁻¹	-0.22	0.04 *	-0.12	0.20 ns

N—nitrogen; * statistically significant at $0.05 < p < 0.01$; ns not significant.

The linear plateau model exhibited the best fit for the actual and estimated KN and EL in response to increasing nitrogen doses (Figure 4a,b). However, the quadratic plateau model exhibited the best fit for the actual and estimated ED in response to increasing nitrogen doses (Figure 4c). For the KN, the linear plateau equation based on the data from the SA was similar to the linear plateau equation based on the estimated KN data

(Figure 4a). Both of them showed that the maximal numbers of kernels, 446 based on the SA, and 444 based on the estimated data, may be obtained with similar amounts of nitrogen—160 and 156 kg N ha⁻¹, respectively. Additional nitrogen did not have an impact on the KN. Both methods showed that the KN attained with 200 kg N ha⁻¹ was statistically higher than the KN with 0, 50, and 100 kg N ha⁻¹. No statistical difference was observed between 150 and 200 kg N ha⁻¹, which led us to the conclusion that the optimal KN per ear may be achieved with an amount between 100 and 150 kg N ha⁻¹.

The maximal actual and estimated EL and ED from the equations (Figure 4b,c) could be acquired with nitrogen doses that were similar to each other. The EL increased up to 150 kg N ha⁻¹, then reached a plateau, with a maximal EL of 21 cm. For the EL, statistical differences were observed between 50 and 150 kg N ha⁻¹, 50 and 200 kg N ha⁻¹, and 50 and 250 kg N ha⁻¹. As expected, both 100 and 150 kg N ha⁻¹ had statistically longer ears in comparison to the controls, which shows that the nitrogen doses required to achieve the optimal EL may be between 100 and 150 kg N ha⁻¹. The nitrogen doses recommended for the optimal ED, based on the statistical differences obtained from the two methods, may be between 50 and 100 kg N ha⁻¹ (Figure 4c). Here, the quadratic plateau model exhibited the best fit with the data, where the maximal actual ED of 4.687 cm was reached with 154 kg N ha⁻¹, and the maximal estimated ED of 4.673 cm was reached with 172 kg N ha⁻¹.

The quadratic plateau model exhibited the best fit with the grain yield, with a maximum of 7.99 t ha⁻¹, which was reached with 148 kg N ha⁻¹ (Figure 4d). Harvest residue (HR) plowing showed statistical significance ($p = 0.04$), whereas nitrogen doses (N) showed high statistical significance ($p < 0.01$) in their effect on the grain yield (S4 File, Supplementary Material). The two-year study presented in [51] did not show the statistical significance of HR on yield and yield components. However, the field where our experiment was placed was established in 1971 as a stationary field trial, which means that HR incorporation from corn, soybean, and wheat occurred as part of a 50 year-long tradition. The short-term effect of crop HR returns on yield observed in [51] was less obvious, possibly since nitrogen fertilizer had a stronger effect than straw return, which can also be seen in some other studies [51,52]. In agreement with [51], we found that there was no statistical difference in grain yield with the highest amounts of nitrogen added. These nitrogen doses intended for optimal yields correspond with results from an 8 year study in which similar doses of this element were used [53]. A quadratic-plateau model has been documented as the best fit for the yield–nitrogen rate relationship [53–55]; after this point, the yield starts to decrease with more than 280 kg N ha⁻¹ [56]. As stated in [57], the yield–nitrogen rate relationship is not expected to decrease immediately after plateauing but remains stable as the nitrogen rate increases. Increments in the nitrogen rate after this point result in increases in per-plant nitrogen uptake (and possibly in plant nitrogen concentrations), but with low or no improvement in per-plant yield. The amounts of nitrogen should be made to equalize the export by harvest, plus a portion of losses, which are also caused by meteorological events. Fertilizers enhance plant growth and therefore the development of the plant biomass. The root biomass is also enhanced along with increased residue amounts during harvest. These higher amounts of organic compounds indicate the presence and activity of microbiota in soil, not only microflora and microfauna but also mesofauna with positive effects on soil structure, and thus humus formation, with the chemical stabilization of the structure and pore formation. The incorporation of high doses of mineral fertilizers into soils and their long-term usage does not always have the expected effect. In the beginning, it may lead to a sudden intensification of microbial processes in the soil, which can be justified if the primary aim is to increase yields. However, it could have various possible consequences, such as disruption of the biological balance; the loss of mineral fertilizers; the degradation of the physical, chemical, and biological properties of the soil; as well as other environmental disturbances, especially in cases of mismanagement and when the best mineral practices are not used [58]. Here, with doses above 150 kg N ha⁻¹, an average yield reduction of 21.1% was observed (Figure 4d). The yield obtained with

150 kg N ha⁻¹ was statistically higher than the control variant and the variant in which 50 kg N ha⁻¹ was added, which means that the nitrogen doses for the optimal yield ranged between 100 and 150 kg ha⁻¹. These amounts of nitrogen were also recommended for the optimal KN and optimal EL values (Figure 4a,b); moreover, these two components were highly correlated (0.99 and 0.97 for estimated and actual obtained traits, Table 4). A very high correlation existed (0.9–1.00) [59] between yield and actual corn ear traits and between yield and estimated ones, and this was statistically significant based on a 5% significance value for Pearson's *r* (0.811) [60]. Based on the research presented in [1], the KN per ear and EL showed a positive and highly significant correlation with grain yield. It was observed that grains yield showed a positive and highly significant correlation with EL (*r* = 0.993 **), ED (*r* = 0.974 **), and KN per ear (*r* = 0.893 **) [61]. This means that we can use DIA to measure corn ear traits obtained from different fertilization variants and to provide nitrogen fertilization amount recommendations for optimal corn yields. Future research on this topic should be based on comparing the DIA and SA of corn ear traits subjected to other independent variables, with variations in resolution and image formats (preferably using RAW images).

Table 4. Correlation matrices for estimated and actual yield components.

(a)				
	Yield	Estimated KN	Estimated EL	Estimated ED
Yield	1.00	0.94	0.96	0.95
Estimated KN	0.94	1.00	0.99	0.98
Estimated EL	0.96	0.99	1.00	0.99
Estimated ED	0.95	0.98	0.99	1.00
(b)				
	Yield	Actual KN	Actual EL	Actual ED
Yield	1.00	0.91	0.95	0.98
Actual KN	0.91	1.00	0.97	0.92
Actual EL	0.95	0.97	1.00	0.95
Actual ED	0.98	0.92	0.95	1.00

(a) correlation matrix between yield and estimated corn ear traits; (b) correlation matrix between yield and actual corn ear traits.

4. Conclusions

Until now, DIA of corn ear traits was primarily used in breeding programs; however, to the best of our knowledge, it has not been used in agrotechnical field trials for comparison between independent factors and variants and for the development of production recommendations based on the results. In contrast to SA for corn ear trait determination in field trials, DIA showed a great reduction in time (being five-times faster), which allowed for the analysis of more plants in specific variants, thus reducing bias. In this study, we presented the results obtained with the lowest resolution possible on the camera that we used. Even with this low-resolution and simple DIA method, a high and statistically significant correlation between automatic and estimated KN, EL, and ED was obtained. For all corn ear traits investigated here, ANOVA for both methods pointed us to the same conclusion, that only nitrogen doses were significantly important for the corn ear traits. Further analysis with the post-hoc testing of nitrogen doses showed only one difference between cases for ED, whereas no discrepancies were seen for KN and EL. Based on these different statistical approaches, we concluded that DIA can be used as a substitute for the SA of corn ear traits in agrotechnical field trials. Results obtained with DIA can serve for the formulation of production recommendations to achieve optimal corn ear traits and, subsequently, optimal corn yields. Future research on this topic should be based on comparing the DIA and SA of corn ear traits obtained from other independent factors and variants, with variations in resolution and image formats, preferably using the RAW image format.

Supplementary Materials: The following supporting information can be downloaded at: <https://www.mdpi.com/article/10.3390/agriculture13030732/s1>, File S1. Macro used for image analysis. File S2. Data used for linear regression, together with output. File S3. Differences and averages of measurements of methods, and linear regression between them. File S4. Data used for ANOVA and post-hoc tests, together with post-hoc test outputs.

Author Contributions: G.J.—writing—review and editing, J.C.—resources, J.V.—investigation, D.L.—supervision, D.D.—formal analysis, investigation, methodology, visualization, writing—original draft. All authors have read and agreed to the published version of the manuscript.

Funding: This research received no external funding.

Institutional Review Board Statement: Not applicable.

Data Availability Statement: The data presented in this study are available on request from the corresponding author.

Acknowledgments: We extend our gratitude to the National Institute of the Republic of Serbia—The Institute of Field and Vegetable Crops in Novi Sad, which enabled research in their field, provided the seed, people, and machinery for necessary agrotechnical operations during the experiment. We extend our gratitude to the Faculty of Agriculture in Novi Sad for providing a kernel counter, precision scale, and students to work. Special thanks to Dušan Petrić for his helpful advices during the preparation of the manuscript.

Conflicts of Interest: The authors declare no conflict of interest.

References

- Inamullah, N.R.; Shah, N.H.; Arif, M.; Siddiq, M.; Mian, I.A. Correlations among grain yield and yield attributes in maize hybrids at various nitrogen levels. *Sarhad J. Agric.* **2011**, *27*, 531–538.
- Santos, T.d.O.; Amaral Junior, A.T.d.; Moulin, M.M. Maize Breeding for Low Nitrogen Inputs in Agriculture: Mechanisms Underlying the Tolerance to the Abiotic Stress. *Stresses* **2023**, *3*, 136–152. [[CrossRef](#)]
- Ma, B.; Wang, J.; Han, Y.; Zhou, C.; Xu, T.; Qu, Z.; Wang, L.; Ma, B.; Yuan, M.; Wang, L.; et al. The Response of Grain Yield and Ear Differentiation Related Traits to Nitrogen Levels in Maize Varieties with Different Nitrogen Efficiency. *Sci. Rep.* **2022**, *12*, 14620. [[CrossRef](#)] [[PubMed](#)]
- Rossini, M.A.; Maddonni, G.A.; Otegui, M.E. Inter-Plant Variability in Maize Crops Grown under Contrasting $n \times$ Stand Density Combinations: Links between Development, Growth and Kernel Set. *Field Crops Res.* **2012**, *133*, 90–100. [[CrossRef](#)]
- Gonzalez, R.C.; Woods, R.E. *Digital Image Processing*, 4th ed.; Pearson: New York, NY, USA, 2018; Chapter 1, p. 18.
- Siddiqi, A.A. *Deep Space Chronicle: A Chronology of Deep Space and Planetary Probes, 1958–2000*; National Aeronautics and Space Administration, Office of External Relations, NASA History Office: Washington, DC, USA, 2002; p. 32.
- Lillesand, T.M.; Kiefer, R.W.; Chipman, J.W. *Remote Sensing and Image Interpretation*; Wiley: Hoboken, NJ, USA, 2015.
- Sarfraz, M. Introductory Chapter: On Digital Image Processing. In *Digital Imaging*; IntechOpen Limited: London, UK, 2020; p. 1.
- Morellos, A.; Pantazi, X.-E.; Moshou, D.; Alexandridis, T.; Whetton, R.; Tziotziou, G.; Wiebensohn, J.; Bill, R.; Mouazen, A.M. Machine Learning Based Prediction of Soil Total Nitrogen, Organic Carbon and Moisture Content by Using Vis-Nir Spectroscopy. *Biosyst. Eng.* **2016**, *152*, 104–116. [[CrossRef](#)]
- Nahvi, B.; Habibi, J.; Mohammadi, K.; Shamsirband, S.; Al Razgan, O.S. Using Self-Adaptive Evolutionary Algorithm to Improve the Performance of an Extreme Learning Machine for Estimating Soil Temperature. *Comput. Electron. Agric.* **2016**, *124*, 150–160. [[CrossRef](#)]
- Johann, A.L.; de Araújo, A.G.; Delalibera, H.C.; Hirakawa, A.R. Soil Moisture Modeling Based on Stochastic Behavior of Forces on a No-till Chisel Opener. *Comput. Electron. Agric.* **2016**, *121*, 420–428. [[CrossRef](#)]
- Kussul, N.; Lavreniuk, M.; Skakun, S.; Shelestov, A. Deep Learning Classification of Land Cover and Crop Types Using Remote Sensing Data. *IEEE Geosci. Remote Sens. Lett.* **2017**, *14*, 778–782. [[CrossRef](#)]
- Kamilaris, A.; Prenafeta-Boldú, F.X. Deep Learning in Agriculture: A Survey. *Comput. Electron. Agric.* **2018**, *147*, 70–90. [[CrossRef](#)]
- Abdullahi, H.S.; Sheriff, R.E.; Mahieddine, F. Convolution Neural Network in Precision Agriculture for Plant Image Recognition and Classification. In Proceedings of the 2017 Seventh International Conference on Innovative Computing Technology (INTECH), Luton, UK, 16–18 August 2017; Institute of Electrical and Electronics Engineers (IEEE): Piscataway, NJ, USA, 2017.
- Ali, I.; Cawkwell, F.; Dwyer, E.; Green, S. Modeling Managed Grassland Biomass Estimation by Using Multitemporal Remote Sensing Data—A Machine Learning Approach. *IEEE J. Sel. Top. Appl. Earth Obs. Remote Sens.* **2017**, *10*, 3254–3264. [[CrossRef](#)]
- Zhang, M.; Li, C.; Yang, F. Classification of Foreign Matter Embedded inside Cotton Lint Using Short Wave Infrared (SWIR) Hyperspectral Transmittance Imaging. *Comput. Electron. Agric.* **2017**, *139*, 75–90. [[CrossRef](#)]
- Binch, A.; Fox, C.W. Controlled Comparison of Machine Vision Algorithms for Rumex and Urtica Detection in Grassland. *Comput. Electron. Agric.* **2017**, *140*, 123–138. [[CrossRef](#)]

18. Pantazi, X.E.; Tamouridou, A.A.; Alexandridis, T.K.; Lagopodi, A.L.; Kashefi, J.; Moshou, D. Evaluation of Hierarchical Self-Organising Maps for Weed Mapping Using UAS Multispectral Imagery. *Comput. Electron. Agric.* **2017**, *139*, 224–230. [CrossRef]
19. FAOSTAT: FAO Statistical Database. Food and Agriculture Organization of the United Nations: Rome, Italy. Available online: <http://faostat.fao.org/default.aspx> (accessed on 19 February 2023).
20. Badr, A.; Sayed-Ahmed, H.; El-Shanshoury, A.; Watson, L. Ancestors of White Clover (*Trifolium repens* L.), as Revealed by Isozyme Polymorphisms. *Theor. Appl. Genet.* **2002**, *106*, 143–148. [CrossRef]
21. Golzarian, M.R.; Frick, R.A.; Rajendran, K.; Berger, B.; Roy, S.; Tester, M.; Lun, D.S. Accurate Inference of Shoot Biomass from High-Throughput Images of Cereal Plants. *Plant Methods* **2011**, *7*, 2. [CrossRef]
22. Miller, N.D.; Haase, N.J.; Lee, J.; Kaeppler, S.M.; Leon, N.; Spalding, E.P. A Robust, High-Throughput Method for Computing Maize Ear, COB, and Kernel Attributes Automatically from Images. *Plant J.* **2016**, *89*, 169–178. [CrossRef] [PubMed]
23. Khaki, S.; Pham, H.; Han, Y.; Kuhl, A.; Kent, W.; Wang, L. Deepcorn: A Semi-Supervised Deep Learning Method for High-Throughput Image-Based Corn Kernel Counting and Yield Estimation. *Knowl.-Based Syst.* **2021**, *218*, 106874. [CrossRef]
24. Zhang, X.; Liu, J.; Song, H. Corn Ear Test Using SIFT-Based Panoramic Photography and Machine Vision Technology. *Artif. Intell. Agric.* **2020**, *4*, 162–171. [CrossRef]
25. Grift, T.E.; Zhao, W.; Momin, M.A.; Zhang, Y.; Bohn, M.O. Semi-Automated, Machine Vision Based Maize Kernel Counting on the Ear. *Biosyst. Eng.* **2017**, *164*, 171–180. [CrossRef]
26. Wu, D.; Cai, Z.; Han, J.; Qin, H. Automatic Kernel Counting on Maize Ear Using RGB Images. *Plant Methods* **2020**, *16*, 79. [CrossRef]
27. Wu, G.; Chen, X.L.; Xie, J.Y.; Zheng, Y.J.; Li, L.H.; Tan, J.S. Design and experiment of automatic variety test system for corn ear. *Trans. Chin. Soc. Agric. Mach.* **2016**, *47* (Suppl. S1), 433–442. (In Chinese)
28. Fromme, D.D.; Spivey, T.A.; Grichar, W.J. Agronomic Response of Corn (*Zea mays* L.) Hybrids to Plant Populations. *Int. J. Agron.* **2019**, *2019*, 3589768. [CrossRef]
29. Zhang, W.; Yu, C.; Zhang, K.; Zhou, Y.; Tan, W.; Zhang, L.; Li, Z.; Duan, L. Plant Growth Regulator and Its Interactions with Environment and Genotype Affect Maize Optimal Plant Density and Yield. *Eur. J. Agron.* **2017**, *91*, 34–43. [CrossRef]
30. Testa, G.; Reyneri, A.; Blandino, M. Maize Grain Yield Enhancement through High Plant Density Cultivation with Different Inter-Row and Intra-Row Spacings. *Eur. J. Agron.* **2016**, *72*, 28–37. [CrossRef]
31. Tiritan, C.S.; Büll, L.T.; Crusciol, C.A.C.; Carmeis Filho, A.C.A.; Fernandes, D.M.; Nascente, A.S. Tillage System and Lime Application in a Tropical Region: Soil Chemical Fertility and Corn Yield in Succession to Degraded Pastures. *Soil Tillage Res.* **2016**, *155*, 437–447. [CrossRef]
32. Zhang, Y.; Wang, R.; Wang, S.; Ning, F.; Wang, H.; Wen, P.; Li, A.; Dong, Z.; Xu, Z.; Zhang, Y.; et al. Effect of Planting Density on Deep Soil Water and Maize Yield on the Loess Plateau of China. *Agric. Water Manag.* **2019**, *223*, 105655. [CrossRef]
33. Battaglia, M.L.; Lee, C.; Thomason, W. Corn Yield Components and Yield Responses to Defoliation at Different Row Widths. *Agron. J.* **2018**, *110*, 210–225. [CrossRef]
34. Pannucci, C.J.; Wilkins, E.G. Identifying and Avoiding Bias in Research. *Plast. Reconstr. Surg.* **2010**, *126*, 619–625. [CrossRef]
35. Stern, R.D. Statistical Procedures in Agricultural Research, by K. A. Gomez and A. A. Gomez. New York, Chichester, Etc.: Wiley (1984), 2nd Edition, Paperback, Pp. 680, Price Not Stated. *Exp. Agric.* **1986**, *22*, 313. [CrossRef]
36. Shafii, B.; Harper, K.C.; McGeehan, S.L. Linear-Plateau Regression Analysis and Its Application to Selenite Adsorption Rate. In Proceedings of the 2nd Annual Conference Proceeding on Applied Statistics in Agriculture, Manhattan, KS, USA, 29 April–1 May 1990; Ag Stat Conference New Prairie Press: Manhattan, KS, USA, 1990.
37. Anderson, R.L.; Nelson, L.A. A Family of Models Involving Intersecting Straight Lines and Concomitant Experimental Designs Useful in Evaluating Response to Fertilizer Nutrients. *Biometrics* **1975**, *31*, 303. [CrossRef]
38. Cerrato, M.E.; Blackmer, A.M. Comparison of Models for Describing; Corn Yield Response to Nitrogen Fertilizer. *Agron. J.* **1990**, *82*, 138–143. [CrossRef]
39. Larson, M.G. Analysis of Variance. *Circulation* **2008**, *117*, 115–121. [CrossRef]
40. Aslam, M.; Albassam, M. Presenting Post Hoc Multiple Comparison Tests under Neutrosophic Statistics. *J. King Saud Univ. Sci.* **2020**, *32*, 2728–2732. [CrossRef]
41. Descriptors for Maize/Descriptores para Maiz/Descripteurs pour...-CGIAR. Available online: http://archive-ecpgr.cgiar.org/fileadmin/bioversity/publications/pdfs/104_Descriptors_for_maize.Descriptores_para_maiz.Descripteurs_pour_le_mais-cache=1415188810.pdf (accessed on 19 February 2023).
42. Makanza, R.; Zaman-Allah, M.; Cairns, J.E.; Eyre, J.; Burgueño, J.; Pacheco, Á.; Diepenbrock, C.; Magorokosho, C.; Tarekne, A.; Olsen, M.; et al. High-Throughput Method for Ear Phenotyping and Kernel Weight Estimation in Maize Using Ear Digital Imaging. *Plant Methods* **2018**, *14*, 49. [CrossRef]
43. Goriewa-Duba, K.; Duba, A.; Wachowska, U.; Wiwart, M. An Evaluation of the Variation in the Morphometric Parameters of Grain of Six Triticum Species with the Use of Digital Image Analysis. *Agronomy* **2018**, *8*, 296. [CrossRef]
44. Lin, L.I.-K. A Concordance Correlation Coefficient to Evaluate Reproducibility. *Biometrics* **1989**, *45*, 255. [CrossRef]
45. Liang, X.; Wang, K.; Huang, C.; Zhang, X.; Yan, J.; Yang, W. A High-Throughput Maize Kernel Traits Scorer Based on Line-Scan Imaging. *Measurement* **2016**, *90*, 453–460. [CrossRef]
46. Vedenov, D.; Pesti, G.M. A Comparison of Methods of Fitting Several Models to Nutritional Response Data. *J. Anim. Sci.* **2008**, *86*, 500–507. [CrossRef] [PubMed]

47. Giavarina, D. Understanding Bland Altman Analysis. *Biochem. Med.* **2015**, *25*, 141–151. [[CrossRef](#)]
48. Wang, C.; Zhang, H.; Yang, L.; Liu, S.; Cao, X. Deep People Counting in Extremely Dense Crowds. In Proceedings of the 23rd ACM International Conference on Multimedia, Brisbane, Australia, 26–30 October 2015; Association for Computing Machinery: New York, NY, USA, 2015.
49. Eagle, A.J.; Bird, J.A.; Horwath, W.R.; Linqvist, B.A.; Brouder, S.M.; Hill, J.E.; Kessel, C. Rice Yield and Nitrogen Utilization Efficiency under Alternative Straw Management Practices. *Agron. J.* **2000**, *92*, 1096–1103. [[CrossRef](#)]
50. Patrício, D.I.; Rieder, R. Computer Vision and Artificial Intelligence in Precision Agriculture for Grain Crops: A Systematic Review. *Comput. Electron. Agric.* **2018**, *153*, 69–81. [[CrossRef](#)]
51. Gao, L.; Li, W.; Ashraf, U.; Lu, W.; Li, Y.; Li, C.; Li, G.; Li, G.; Hu, J. Nitrogen Fertilizer Management and Maize Straw Return Modulate Yield and Nitrogen Balance in Sweet Corn. *Agronomy* **2020**, *10*, 362. [[CrossRef](#)]
52. Phongpan, S.; Mosier, A.R. Effect of Rice Straw Management on Nitrogen Balance and Residual Effect of Urea-n in an Annual Lowland Rice Cropping Sequence. *Biol. Fertil. Soils* **2002**, *37*, 102–107. [[CrossRef](#)]
53. Schwalbert, R.; Amado, T.J.C.; Horbe, T.A.; Stefanello, L.O.; Assefa, Y.; Prasad, P.V.V.; Rice, C.W.; Ciampitti, I.A. Corn Yield Response to Plant Density and Nitrogen: Spatial Models and Yield Distribution. *Agron. J.* **2018**, *110*, 970–982. [[CrossRef](#)]
54. Roberts, D.F.; Ferguson, R.B.; Kitchen, N.R.; Adamchuk, V.I.; Shanahan, J.F. Relationships between Soil-Based Management Zones and Canopy Sensing for Corn Nitrogen Management. *Agron. J.* **2012**, *104*, 119–129. [[CrossRef](#)]
55. Scharf, P.C.; Kitchen, N.R.; Sudduth, K.A.; Davis, J.G.; Hubbard, V.C.; Lory, J.A. Field-Scale Variability in Optimal Nitrogen Fertilizer Rate for Corn. *Agron. J.* **2005**, *97*, 452–461. [[CrossRef](#)]
56. Eck, H.V. Irrigated Corn Yield Response to Nitrogen and Water. *Agron. J.* **1984**, *76*, 421–428. [[CrossRef](#)]
57. Ciampitti, I.A.; Vyn, T.J. Physiological Perspectives of Changes over Time in Maize Yield Dependency on Nitrogen Uptake and Associated Nitrogen Efficiencies: A Review. *Field Crops Res.* **2012**, *133*, 48–67. [[CrossRef](#)]
58. Latkovic, D.; Maksimovic, J.; Dinic, Z.; Pivic, R.; Stanojkovic, A.; Stanojkovic-Sebic, A. Case Study upon Foliar Application of Biofertilizers Affecting Microbial Biomass and Enzyme Activity in Soil and Yield Related Properties of Maize and Wheat Grains. *Biology* **2020**, *9*, 452. [[CrossRef](#)]
59. Asuero, A.G.; Sayago, A.; González, A.G. The Correlation Coefficient: An Overview. *Crit. Rev. Anal. Chem.* **2006**, *36*, 41–59. [[CrossRef](#)]
60. Snedecor, G.W. *Statistical Methods: Applied to Experiments in Agriculture and Biology*, 4th ed.; Iowa State College Press: Ames, IA, USA, 1950.
61. Chetan, H.T.; Potdar, M.P.; Nadagouda, B.T.; Patil, P.L.; Patil, C.R. Correlations among Grain Yield and Yield Attributes in Maize Hybrids as Influenced by Site Specific Nutrient Management (SSNM). *Int. J. Curr. Microbiol. Appl. Sci.* **2017**, *6*, 2292–2296. [[CrossRef](#)]

Disclaimer/Publisher’s Note: The statements, opinions and data contained in all publications are solely those of the individual author(s) and contributor(s) and not of MDPI and/or the editor(s). MDPI and/or the editor(s) disclaim responsibility for any injury to people or property resulting from any ideas, methods, instructions or products referred to in the content.